

1 Title: Identifying the essential genes of *Mycobacterium avium* subsp. *hominissuis* with Tn-Seq using a
2 rank-based filter procedure.

3 Running Title: Essential Genes of *Mycobacterium avium*

4 Authors: William M. Matern^{a,b,c}, Robert L. Jenquin^c, Joel S. Bader^{b,c#}, Petros C. Karakousis^{c,d#}

5 Affiliations:

6 a – Department of Biomedical Engineering, Johns Hopkins School of Medicine, Baltimore, MD

7 b – High-Throughput Biology Center, Johns Hopkins School of Medicine, Baltimore, MD

8 c – Center for Tuberculosis Research, Department of Infectious Diseases, Johns Hopkins School of
9 Medicine, Baltimore, MD

10 d – Department of International Health, Johns Hopkins Bloomberg School of Public Health, Baltimore,
11 MD

12 # - joel.bader@jhu.edu

13 # - petros@jhmi.edu

14

15 **Abstract:**

16 *Mycobacterium avium* (Mav) is increasingly recognized as a significant cause of morbidity, particularly in
17 elderly patients or those with immune deficiency or underlying structural lung disease. Generally, Mav
18 infection is treated with 2-3 antimicrobial drugs for at least 12 months. Identification of genes essential
19 for Mav growth may yield novel strategies for improving curative therapy. We have generated
20 saturating genome-wide transposon mutant pools in a commonly used laboratory strain of
21 *Mycobacterium avium* subsp. *hominissuis* (MAC109) and developed a computational technique for
22 classifying annotated genomic features as essential (ES), growth defect (GD), growth advantage (GA), or
23 no-effect (NE) based on the *in vitro* effect of disruption by transposon. We identified 270 features as ES
24 with 230 of these overlapping with ES features in *Mycobacterium tuberculosis*. These results may be
25 useful for identifying drug targets or for informing studies requiring genetic manipulation of
26 *Mycobacterium avium*, which should seek to avoid disrupting ES features to ensure bacterial viability.

27

28 **Importance:**

29 *Mycobacterium avium* subsp. *hominissuis* is an emerging cause of morbidity in vulnerable populations in
30 many countries. It is known to be particularly difficult to treat, often requiring years of antibiotic
31 therapy. In this study we report the genes of *Mycobacterium avium* subsp. *hominissuis* that are required
32 for the organism to grow *in vitro*. Our findings may help guide future research into identifying new drugs
33 to improve the treatment of this serious infection.

34

35 **Introduction:**

36 The genus *Mycobacteria* contains a variety of difficult-to-treat pathogens, frequently associated
37 with pulmonary disease. One of these pathogens, *Mycobacterium avium* (Mav), is an opportunistic
38 pathogen associated with significant morbidity in the elderly and in patients with underlying lung
39 disease ^{1,2} as well as increased mortality in patients with AIDS ³. Similar to other mycobacteria, Mav is
40 often difficult to treat effectively with existing antibiotic combinations. Current antibiotic regimens
41 require a median of 5 months to convert the sputum to a culture-negative state ⁴, with current
42 guidelines suggesting these infections be treated for at least 1 year after sputum conversion ⁵.
43 Furthermore, a large fraction of patients fail to convert after 1 year of therapy ⁴. Patients could greatly
44 benefit from new therapeutic approaches with greater efficacy and reduced duration.

45 Transposon sequencing (e.g., TraDIS ⁶, Tn-Seq ⁷, INseq ⁸) has been extensively used to profile
46 haploid genomes and identify gene disruptions that affect bacterial growth under various conditions. Of
47 potential interest in drug development are those drug targets which profoundly disrupt growth on rich
48 media (i.e., “essential” genes). In the current study, we have identified genes critical for Mav growth *in*
49 *vitro* with the goal of informing future research in Mav pathogenesis and drug development. In order to
50 make gene essentiality predictions, we developed a new statistical approach for calling genes based on
51 ranking the read counts from each mutant and applied this to new Tn-Seq data. We report our
52 predictions of the essential genes of Mav and compare these with the predicted set of essential genes in
53 the closely related human pathogen, *Mycobacterium tuberculosis*.

54

55 **Results:**

56 **Constructing Genome-wide Transposon Mutant Pools in *Mycobacterium avium***

57 To identify a suitable strain of Mav for genome-wide mutagenesis, we evaluated the ability of
58 the Himar1 transposon (delivered via Φ mycomarT7⁹), which inserts randomly into thymine-adenine
59 dinucleotide (TA sites), to transform common laboratory strains. Transformation efficiency and
60 spontaneous resistance rate (background) were estimated via CFU counts and are provided in Table S1.
61 Of the 5 strains tested, MAC109 was observed to have the highest transformation efficiency with only
62 ~1% background. Therefore, we decided to proceed with transposon mutagenesis with this strain. Upon
63 transformation, we estimated each of our five independent MAC109 transposon mutant libraries
64 contained between $2.2 - 4.4 \times 10^5$ unique insertion events, for a combined total of 1.2×10^6 unique
65 events with ~2% background. To assist with analysis, we recently provided the genome of this strain
66 which was found to contain a 5,188,883 bp chromosome and two plasmids (pMAC109a and pMAC109b)
67 of lengths 147,100 bp and 16,516 bp, respectively¹⁰. There were 60,129 unique TA sites across the entire
68 genome.

69

70 **Confirmation of site bias**

71 It was previously shown that the Himar1 transposon/transposase system has a reduced rate of
72 insertion in sites containing the sequence motif [CG]GNTANC[CG]⁷. Indeed, our results confirm that
73 insertion into these low permissibility sites is much less likely than other sites (Figure 1). Although our
74 approach was able to disrupt nearly all possible insertion sites in the genome not matching this motif
75 (i.e., achieving saturation), a substantial fraction of the low permissibility sites in the chromosome were
76 unoccupied in all five libraries. This effect was less apparent in the plasmids, likely due to their multiple
77 copy number¹⁰.

78

79 **Annotation of MAC109 Genetic Features**

80 Our analysis method classified 270 features as ES, 489 features as GA, 1267 features as GD out
81 of 5091 total annotated features. 73 features contained no TA sites and 9 features only contained TA
82 sites shared with another feature. Therefore, these 82 features could not be evaluated with the Himar1
83 system. Our method classified 259 annotated coding sequences, 8 tRNAs, and 2 rRNAs as well as the
84 only annotated tmRNA as essential. No annotated pseudogenes were labelled as essential though a
85 minority of them were found to affect growth (i.e. were GA/GD). A summary of classifications by feature
86 type is provided in Table 1 with classifications for individual features provided in Table S2. Table S3
87 provides these classifications merged with the raw read count data. Interestingly, our method identified
88 3 annotated coding sequences in pMAC109a and 1 coding sequence in pMAC109b as essential.

89

90 **Comparison of annotations with previously published transposon-based annotations**

91 We compared the results of our analysis method applied to a previously published Tn-Seq
92 dataset using *Mycobacterium tuberculosis* strain H37Rv⁷. All genes labelled as “ESD” (containing an
93 essential domain) in the previously published dataset were considered essential for comparison. Figure
94 2 shows the overlap in the predicted essential coding sequences (CDS) from each method (RNA and
95 other features excluded). Overall, there was good agreement between each method though our method
96 appears to be somewhat more sensitive for essential gene detection than the previous method at this
97 sample size. Upon inspection it was observed that the essential genes unique to our method contained a
98 significant number of sites with zero or very few insertions, but these sites were interspersed among
99 sites containing larger numbers of reads. This fits with expectations that the hidden Markov model used
100 previously is sensitive primarily to multiple adjacent sites with low read counts, whereas our method is
101 sensitive to the number of sites per gene regardless of adjacency.

102

103 **Discussion:**

104 We identified 230 genes as essential in both Mav and Mtb (Table S5). These may represent
105 particularly good targets for drug development, as inhibitors of a gene product are likely to be effective
106 against a close ortholog. As expected, a number of well-demonstrated targets are present. This includes
107 the targets of the mycobacterial drugs cycloserine (alanine racemase, D-alanine – D-alanine ligase),
108 rifamycins (RNA polymerase beta subunit), macrolides (50S ribosome), aminoglycosides (30S ribosome),
109 fluoroquinolones (type IV topoisomerases and gyrases), bedaquiline (ATP synthase), and ethambutol
110 (arabinosyltransferase). Additional compounds that have been reported to have some activity against
111 mycobacteria include tryptophan synthase inhibitors ¹¹, ClpP inhibitors ¹², and Rho inhibitors (albeit only
112 shown to be effective through genetic manipulation) ¹³. A brief literature search also reveals many
113 compounds that inhibit non-mycobacterial orthologs of these genes but appear to lack published results
114 for killing activity in mycobacteria including inhibitors of GroEL ¹⁴, RibBA ¹⁵, SecA ¹⁶, and LigA ^{17,18}. It is
115 thus apparent that many opportunities are available for targeting these overlapping essential
116 mycobacterial genes.

117 Our analysis classified four protein-coding genes on the two plasmids as essential (3 on
118 pMAC109a and 1 on pMAC109b). This was somewhat surprising, as these plasmids have multiple copies
119 per cell, and a disruption of a single gene copy should, in theory, be complemented by other copies. We
120 used NCBI BLAST to find homologs of these genes. DFS55_24645 (on pMAC109a) and DFS55_25425 (on
121 pMAC109b) are homologous to Rep, a protein critical for the replication of plasmids. Thus, one possible
122 explanation for the essentiality of these Rep homologs is that plasmid copy number will decrease in
123 daughter cells inheriting the plasmid (with no plasmid replication possible in a cell with all copies
124 containing disrupted Rep). This is a strong selective pressure against the mutant plasmid. DFS55_14680
125 (on pMAC109a) is a ParA homolog. ParA controls the distribution of plasmids to daughter cells such that

126 cells inherit the plasmid more equally. It is not immediately apparent how a more random distribution
127 of the plasmids due to disruption of ParA would lead to a growth defect. Lastly, DFS55_24600 (on
128 pMAC109a) is a hypothetical protein also classified as essential. It lacks a paralog in the MAC109
129 chromosome and an ortholog in *Mycobacterium avium* strain 104 (which does not contain plasmids).
130 Thus, it appears to be non-essential for the *Mycobacterium avium* subsp. *hominissuis* pangenome.
131 DFS55_24600 is homologous to Rv3081 from H37Rv and our analysis identified Rv3081 as “GD”
132 (approximately 0.25 Relative Fitness). It is also apparent from examining the raw Tn-seq read counts
133 (Table S3) that transposon insertion in the beginning of this gene does not have a profound effect on
134 growth rate in MAC109 (this trend is less clear in H37Rv). Given these observations we can only
135 speculate that this gene is addictive in MAC109 (and weakly addictive in H37Rv) – and may represent a
136 toxin-antitoxin fusion with the toxin domain near the N-terminus. Future work could clone DFS55_24600
137 into an episomal (non-integrating) mycobacterial shuttle vector (such as pPB10) and examine the
138 retention of the episome with and without this gene in the absence of antibiotic selection. Additionally,
139 an attempt could be made to isolate a MAC109 mutant cured of pMAC109a.

140 Our analysis method has several advantages over other methods, including its anticipated high
141 robustness as the result of using the zero-inflated negative-binomial to model read counts, which can
142 more accurately account for non-saturating libraries, as these have a high probability of a site having no
143 observed insertions. This may be especially important for transposons which cannot easily achieve
144 saturation without very large numbers of transformants (due to lack of the strict TA site bias of *Himar1*),
145 such as the Tn5 system ¹⁹. Also, we have fully exploited the statistical independence of samples, which
146 increases our statistical power. Other models, such as hidden Markov models, generally pool samples,
147 limiting the usefulness of having biological replicates. However, our method also has limitations. Using
148 our collected data, we detected a somewhat low number of essential features in MAC109 relative to
149 H37Rv (270 and 738, respectively) despite evidence that the genome was saturated with insertions

150 (Figure 1). Most likely, this is due to our somewhat low sample size (5 independent libraries). Therefore,
151 we believe that sequencing additional independent transposon mutant libraries could significantly
152 increase the statistical power to detect essential genes in MAC109, particularly for features with fewer
153 insertion sites. A previous study ⁷ used 14 independent libraries for H37Rv, which seemed to give our
154 method good statistical power and may be a useful sample-size target for future studies. Additionally,
155 while our method can correctly handle sites with low rates of insertion (e.g., [CG]GNTANC[CG]) it is
156 possible that additional such sites exist that have not yet been defined. Defining the sites with low rates
157 of insertion is especially important to avoid features falsely classified as essential.

158 In conclusion, we have generated genome-wide transposon mutant pools in *Mycobacterium*
159 *avium* strain MAC109, collected sequencing data, and used a novel approach for annotating genes based
160 on this data. We find that these pools are nearly saturated with transposon insertions, although not at
161 low permissibility sites previously shown to have a reduced insertion rate. Our analysis identified the
162 essential genes of MAC109 and we suggested explanations for the apparent detection of essential genes
163 in the plasmids. We recommend that additional independent MAC109 transposon mutant libraries be
164 collected, which we expect will greatly increase sensitivity. Future work could confirm our growth
165 predictions by adapting the existing mycobacterial dCas9 knockdown system ²⁰ to *Mycobacterium avium*
166 and measuring the impact of gene knockdown on bacterial growth rate.

167

168 **Materials and Methods:**

169 **Strains**

170 MAC109, MAC104, OSU3388 were a gift from Dr. Luiz Bermudez (Oregon State University).
171 MAC101 (Chester, ATCC 700898) was a gift from Dr. Eric Nuermberger (Johns Hopkins School of

172 Medicine). Individual colonies of each strain were isolated and regrown to make stocks used in the
173 described experiments. MAC101 was seen to form both translucent and opaque colonies. Both an
174 opaque (MAC101o) and a translucent (MAC101t) colony were isolated and used for stocks.

175 Φ mycomarT7 was propagated and titered as previously described²¹. Final titers used for
176 transformations exceeded 10^{11} PFUs/mL.

177

178 **Media and Buffers**

179 To make 7H11 agar 10.25 grams of 7H11 w/o Malachite Green powder (HiMedia Cat No. 511A)
180 was added to 450mL deionized water. 5mL 50% glycerol was then added before autoclaving. Hot agar
181 was cooled to 55°C before addition of 50mL OADC enrichment and 1.25mL 20% Tween-80.

182 To make 7H9/10% OADC: 2.35g 7H9 powder was added to 450mL deionized water. After sterilization
183 (via autoclaving at 121°C or by passing through a 0.22um filter) 50mL of OADC enrichment (Becton-
184 Dickinson) was added. Unless otherwise specified, no Tween-80 or glycerol was included.

185 To make 7H9/50% OADC: Recipe identical to 7H9/10% OADC but using 250mL water and 250mL OADC.

186 To make PBS-Tw: 1.25mL filter-sterilized 20% Tween-80 was added to 500mL sterile PBS.

187 To make MP Buffer: 50mM Tris-HCl (pH 7.5), 150mM NaCl, 10mM MgSO₄, 2mM CaCl₂. Autoclave
188 individual components before combining.

189

190 **Testing of transformation efficiency of Mav strains**

191 Five strains of Mav (MAC109, MAC104, OSU3388, MAC101o, MAC101t) were tested for
192 transformation by Φ mycomarT7. For transformation, strains were grown in 150mL of 7H9/10% OADC.

193 After OD of each strain reached 0.32 – 0.89, 100mL of cultures were equally split into two 50mL conical
194 tubes. Bacteria were pelleted via centrifugation and resuspended in 10mL MP buffer. Bacteria were
195 pelleted again via centrifugation and resuspended in 4.5mL MP Buffer. 0.5mL of MP Buffer (negative
196 control) or Φ mycomarT7 stock (approximately 10:1, phage:bacteria) was added to each tube. Tubes
197 were incubated for two days shaking at 37°C. Bacteria were then pelleted via centrifugation and
198 resuspended in PBS-Tw (phosphate-buffered saline containing 0.05% Tween-80). Bacteria were then
199 spun down again and resuspended in 1mL of PBS-Tw. Transformed bacteria and negative control for
200 each strain were then diluted in PBS-Tw and plated on 7H11 with and without 50ug/mL kanamycin for
201 titration.

202

203 **Generation of transposon mutant libraries in MAC109**

204 In preliminary experiments, we found that MAC109 growth increased at higher concentrations
205 of OADC. We suspect the oleic acid in OADC is the key to achieving this, based on previous reports ²². 5
206 independent transposon mutant pools were generated. MAC109 was grown in 700mL 7H9/50%OADC to
207 OD 2.1 in two 1.5L roller bottles shaking at 37°C. Based on previous results (data not shown) we
208 estimated the initial bacterial density based on optical density to be 4×10^8 CFUs/mL for calculation of
209 volume of phage stocks. Bacteria were aliquoted to 12-50mL conical tubes and centrifuged (2000g for 5
210 minutes) and supernatant removed. 5mL MP Buffer was added to each tube and bacterial pellet was
211 resuspended. Pairs of tubes were pooled yielding 6-10mL aliquots. Samples were then centrifuged
212 (2000g for 5 minutes) and supernatant removed. Phage (10:1, phage:bacteria) was then added to all
213 tubes except no-vector control. MP Buffer was added to all tubes to a final volume of 5mL and bacterial
214 pellets were dispersed via pipette. Bacterial/phage mixtures were then placed on a shaker incubator
215 (37°C) for two days. Tubes were then centrifuged (2000g for 5 minutes) and supernatant removed. 10mL

216 PBS-Tw was then added and the bacterial pellet was dispersed via pipette. Tubes were then spun down
217 again (2000g for 5 minutes), supernatant removed, and 1 mL of PBS-Tw was used to resuspend pellets.

218 50uL of each tube of washed transformants (or no-vector control) were diluted and plated on
219 7H11 plates, with or without 50ug/mL kanamycin, to determine transformation efficiency and
220 background resistance. The remainder of the cultures were plated on 7H11 containing 50ug/mL
221 kanamycin in Pyrex baking dishes (15" x 10", 500mL agar per dish, 1 tube per dish). After 7-10 days
222 colonies were scraped from each dish and dispersed in fresh 7H9 broth and frozen in aliquots at -80°C
223 for later use.

224 DNA was extracted from one aliquot of each transposon mutant pool using a previously
225 described gDNA extraction protocol for short read sequencing¹⁰. We adapted a previously published
226 library prep protocol²³ to prepare libraries for sequencing. Adaptations include the use of magnetic
227 beads for purification and library size selection as well as changes to PCR conditions (for details see Text
228 S1). Libraries were sequenced (2x75bp) on an Illumina HiSeq 2500 by the Johns Hopkins GRCF High
229 Throughput Sequencing Center. 5 independent libraries were sequenced yielding between 2,194,085 –
230 4,381,545 reads per library for a total of 18,197,728 paired-end reads.

231

232 **Raw Data processing**

233 We previously showed that the MAC109 genome contains two plasmids in addition to the
234 bacterial chromosome. We adapted the TRANSIT pre-processor (tpp)²⁴ to allow for mapping to multiple
235 contigs. These changes were included in the release of TRANSIT/tpp v2.4.1. We used tpp v2.4.1 to map
236 all reads to the MAC109 genome. Command for processing raw reads: tpp -himar1 -bwa -bwa-aln -
237 ref MAC109.gb -replicon-ids “CP029332,CP029333,CP029334” -reads1 TnPool_1.fastq -reads2

238 TnPool_2.fastq -window-size 6 -primer AACCTGTTA -mismatches 2. After PCR duplicate removal, a total
239 of 10,597,261 unique reads mapped to the genome and were used for analysis.

240

241 **Statistical Analysis**

242 We use a previously suggested labelling scheme²⁵ to annotate each gene of MAC109. A gene is
243 labelled NE (No Effect) if a transposon insertion in any of its potential insertion sites causes no effect on
244 growth. A gene is labelled GD (Growth Defect) if it contains at least one insertion site such that upon
245 transposon insertion it results in a decrease in bacterial growth. A gene is labelled GA (Growth
246 Advantage) if it contains at least one insertion site such that upon transposon insertion it results in an
247 increase in bacterial growth. A gene is labelled ES (essential) if it contains at least one insertion site such
248 that upon transposon insertion it results in a large loss in viability.

249 To annotate the MAC109 genome, we have designed a robust procedure. Some additional
250 details of this method are provided in the supplement (Text S2). At a conceptual level, our analysis
251 pipeline proceeds in two steps. First, insertion sites without a growth defect are approximately
252 identified with a rank-based filter procedure. Second, the counts at the insertion sites identified by the
253 filter are assumed to approximate the null distribution and used for statistical hypothesis testing. For
254 identification of ES genes, the approximate null distribution is fit to a zero-inflated negative binomial
255 distribution (using maximum likelihood estimation) which is then scaled and used for hypothesis testing.
256 For identifying the GD and GA sites, the empirical cumulative distribution function is used for hypothesis
257 testing. Stouffer's method is used to combine p-values from multiple replicates and multiple sites.
258 Lastly, multiple hypothesis correction is performed (Benjamini-Hochberg for ES, Bonferroni for GD/GA
259 testing).

260 *Relative Fitness*

261 The fitness, relative to wildtype, resulting from disruption of a particular gene is approximated
262 as follows. First, the mean of the read counts at each insertion site is calculated across samples. The site
263 fitness is calculated as the mean read count of each site divided by the median across all sites (i.e.,
264 samples are normalized to the median). Finally, each gene is assigned a Relative Fitness equal to the
265 median of the site fitness for all sites contained in the gene.

266

267 *Rank-based filter procedure*

268 We assumed that all mutants with a transposon insertion at the same site will have identical
269 growth rates (i.e., the growth rate is entirely defined by the insertion site). We also assumed that not
270 more than 40% of insertion mutants would have a growth defect and not more than 15% of mutants
271 would have a growth advantage (and therefore at least 45% of mutants would have a growth rate that is
272 identical to wildtype). We selected these thresholds based on previous predictions in *Mycobacterium*
273 *tuberculosis*⁷ suggesting that 15% of insertion sites cause a growth defect and 8% cause a growth
274 advantage. We have added a large margin of error to ensure conservatism.

275 Note that if some of the identities of insertions mutants with growth rates identical to wildtype
276 were known ahead of time we could simply use the distribution of the reads at these sites to train a null
277 model to test the other sites. This is the intuition behind our rank-based filter procedure. However, as
278 the identities of the insertion sites with no effect on growth rate are unknown we use an approximation.
279 For each of J transposon pools (replicates) we compute the rank of the read count at each site
280 (averaging identical ranks) in the other $J-1$ samples. For each site, we then take the average of these $J-1$
281 ranks across samples. Lastly, we order the average rank from least to greatest and remove the smallest
282 40% and greatest 15% (removing additional sites with ties at the threshold), leaving only \sim 45% of the
283 original insertion sites. The read counts from these remaining \sim 45% of sites will be distributed

284 approximately the same as an insertion site with no effect on growth. Additionally, previous literature
285 suggests that the *Himar1* transposon is biased against insertion sites with the motif (GC)GN TANC(GC)⁷.
286 Therefore, we separately apply the above rank-based filter to the read count data collected from these
287 sites.

288 To demonstrate the correctness of our rank-based filter procedure we utilized simulated data.
289 Briefly, read counts from 39,000 insertion mutants without a defect were simulated as a negative
290 binomial distribution with mean 35 and dispersion 3.0. These parameters are roughly those found by
291 fitting real data (fitting procedure described below). Additionally, read counts from 15,000 mutants with
292 a growth defect were simulated with a mean of between 0 and 0.67 times that of a no defect mutant
293 using the negative binomial distribution with an identical dispersion. The mean multiplier was chosen
294 for these mutants by uniform sampling between these bounds. Lastly, read counts from 6,000 mutants
295 with a growth advantage were simulated using 1.5 to 4 times the null mean (uniformly distributed) and
296 identical dispersion. Combining these 3 groups of samples provided a simulated transposon mutant
297 library. 5 and 50 independent simulated transposon mutant libraries were generated. The rank-based
298 filter procedure described above was then applied to the resulting datasets. Q-q plots provided in
299 Figures S1B and S1D comparing the theoretical distribution to the unfiltered and filtered empirical cdfs
300 show that the filter procedure improves accuracy. Increased sample size also improves accuracy, as
301 expected.

302 *Hypothesis Testing for Essentiality (ES)*

303 To classify a gene as ES, we performed statistical hypothesis testing. The read counts from the
304 insertion sites identified by the rank-based filter are used to fit a zero-inflated negative binomial
305 distribution (See Text S2 for definition). Fitting is done by maximizing the likelihood with L-BFGS-B as
306 implemented in `scipy.optimize` (Scipy v1.2.1). Using the fit distribution, we then create a new

307 “borderline ES” distribution by scaling the mean of the negative binomial distribution to 5% of the
308 original, keeping the dispersion and zero inflation component constant. We use this borderline
309 distribution to do statistical hypothesis testing on the read counts from each of the sites using the lower
310 tail probability as the p-value. This means that a gene whose insertion gives 5% of WT growth is unlikely
311 to be called ES. While the particular threshold we have chosen (5% of wildtype growth) is somewhat
312 arbitrary, we feel it is both small enough to ensure mutants labelled ES are highly defective but not so
313 small so as to have no hope of classifying highly defective mutants as ES.

314 To pool essential p-values across samples, we used the one-tailed Stouffer’s method at each
315 site. To pool p-values across insertion sites within a gene we use the truncated product method²⁶ with a
316 truncation threshold of 0.5 ($\tau < 0.5$). TPM provides a principled approach for limiting the effect of sites
317 with no associated growth defect which would otherwise greatly inflate the p-values (such as those sites
318 at the C-terminus of the gene which may not disrupt the function of the protein). We then control the
319 False Discovery Rate (FDR) using the Benjamini-Hochberg procedure (FDR < 0.01).

320

321 *GD/GA Hypothesis Testing*

322 To classify a gene as GD or GA, we performed statistical hypothesis testing. We utilized the read
323 counts for insertion sites identified by the rank-based filter to form an approximate null distribution and
324 used the empirical cumulative distribution function (ecdf) to compute p-values. We generated a
325 separate ecdf for low permissibility sites. We also generated separate ecdfs for each contig as
326 sequencing depth varied greatly between contigs (due to multiple copy-number plasmids). The exact p-
327 value computation, which ensures p-values are continuously distributed, is described in detail in the
328 supplement. For a particular insertion site, the p-values from each sample were pooled using the one-
329 tailed Stouffer’s method. The resulting pooled p-values from all insertion sites within the same gene

330 were then pooled using the two-tailed Stouffer's method. For declaring genes as GA or GD we set the p-
331 value threshold to allow only a single (expected) false discovery after 5009 tests, corresponding to a
332 single-test p-value of approximately 0.0002. A gene was declared GD if its Relative Fitness was less than
333 2/3 and was statistically significant ($p < 0.0002$). Similarly, a gene was declared GA if its Relative Fitness
334 was greater than 1.5 and was statistically significant at the same threshold. Note that if a gene meets
335 the criteria for both the GD and ES label then it is given the ES label only. If it meets the ES criteria but
336 not the GD label it is given the NE label.

337

338 **Data and Source Code Availability**

339 We have made efforts to enable others to reproduce the major results of this paper from the
340 raw data. Scripts and instructions for use are provided at GitHub
341 (https://github.com/joelbader/essential_genes)²⁷. Raw data is provided in NCBI's SRA under accession
342 number: PRJNA527645.

343

344 **Acknowledgements:**

345 This publication was made possible by support from the Sherrilyn and Ken Fisher Center for
346 Environmental Infectious Diseases, Division of Infectious Diseases of the Johns Hopkins University
347 School of Medicine. Its contents are solely the responsibility of the authors and do not necessarily
348 represent the official view of the Fisher Center or Johns Hopkins University School of Medicine.

349

350 We are grateful to Dr. Luiz Bermudez for providing strains and advice during this project.

351

353 **References**

354 1. Prevots, D. R. *et al.* Nontuberculous mycobacterial lung disease prevalence at four integrated health
355 care delivery systems. *Am. J. Respir. Crit. Care Med.* **182**, 970–976 (2010).

356 2. Diel, R., Lipman, M. & Hoefsloot, W. High mortality in patients with *Mycobacterium avium* complex
357 lung disease: a systematic review. *BMC Infect. Dis.* **18**, 206 (2018).

358 3. Chaisson, R. E., Moore, R. D., Richman, D. D., Keruly, J. & Creagh, T. Incidence and natural history of
359 *Mycobacterium avium*-complex infections in patients with advanced human immunodeficiency virus
360 disease treated with zidovudine. The Zidovudine Epidemiology Study Group. *Am. Rev. Respir. Dis.*
361 **146**, 285–289 (1992).

362 4. Griffith, D. E. *et al.* Semiquantitative Culture Analysis during Therapy for *Mycobacterium avium*
363 Complex Lung Disease. *Am. J. Respir. Crit. Care Med.* **192**, 754–760 (2015).

364 5. Griffith, D. E. *et al.* An official ATS/IDSA statement: diagnosis, treatment, and prevention of
365 nontuberculous mycobacterial diseases. *Am. J. Respir. Crit. Care Med.* **175**, 367–416 (2007).

366 6. Langridge, G. C. *et al.* Simultaneous assay of every *Salmonella Typhi* gene using one million
367 transposon mutants. *Genome Res.* **19**, 2308–2316 (2009).

368 7. DeJesus, M. A. *et al.* Comprehensive Essentiality Analysis of the *Mycobacterium tuberculosis*
369 Genome via Saturating Transposon Mutagenesis. *MBio* **8**, (2017).

370 8. Goodman, A. L. *et al.* Identifying genetic determinants needed to establish a human gut symbiont in
371 its habitat. *Cell Host Microbe* **6**, 279–289 (2009).

372 9. Sassetti, C. M., Boyd, D. H. & Rubin, E. J. Comprehensive identification of conditionally essential
373 genes in mycobacteria. *Proc. Natl. Acad. Sci. U.S.A.* **98**, 12712–12717 (2001).

374 10. Matern, W. M., Bader, J. S. & Karakousis, P. C. Genome analysis of *Mycobacterium avium* subspecies
375 *hominissuis* strain 109. *Sci Data* **5**, 180277 (2018).

376 11. Abrahams, K. A. *et al.* Inhibiting mycobacterial tryptophan synthase by targeting the inter-subunit
377 interface. *Sci Rep* **7**, 9430 (2017).

378 12. Compton, C. L., Schmitz, K. R., Sauer, R. T. & Sello, J. K. Antibacterial activity of and resistance to
379 small molecule inhibitors of the ClpP peptidase. *ACS Chem. Biol.* **8**, 2669–2677 (2013).

380 13. Botella, L., Vaubourgeix, J., Livny, J. & Schnappinger, D. Depleting *Mycobacterium tuberculosis* of
381 the transcription termination factor Rho causes pervasive transcription and rapid death. *Nat
382 Commun* **8**, 14731 (2017).

383 14. Kunkle, T. *et al.* Hydroxybiphenylamide GroEL/ES Inhibitors Are Potent Antibacterials against
384 Planktonic and Biofilm Forms of *Staphylococcus aureus*. *J. Med. Chem.* (2018).
385 doi:10.1021/acs.jmedchem.8b01293

386 15. Islam, Z., Kumar, A., Singh, S., Salmon, L. & Karthikeyan, S. Structural basis for competitive inhibition
387 of 3,4-dihydroxy-2-butanone-4-phosphate synthase from *Vibrio cholerae*. *J. Biol. Chem.* **290**, 11293–
388 11308 (2015).

389 16. Jin, J. *et al.* SecA inhibitors as potential antimicrobial agents: differential actions on SecA-only and
390 SecA-SecYEG protein-conducting channels. *FEMS Microbiol. Lett.* **365**, (2018).

391 17. Brötz-Oesterhelt, H. *et al.* Specific and potent inhibition of NAD⁺-dependent DNA ligase by
392 pyridochromanones. *J. Biol. Chem.* **278**, 39435–39442 (2003).

393 18. Gong, C., Martins, A., Bongiorno, P., Glickman, M. & Shuman, S. Biochemical and genetic analysis of
394 the four DNA ligases of mycobacteria. *J. Biol. Chem.* **279**, 20594–20606 (2004).

395 19. Lodge, J. K., Weston-Hafer, K. & Berg, D. E. Transposon Tn5 target specificity: preference for
396 insertion at G/C pairs. *Genetics* **120**, 645–650 (1988).

397 20. Rock, J. M. *et al.* Programmable transcriptional repression in mycobacteria using an orthogonal
398 CRISPR interference platform. *Nat Microbiol* **2**, 16274 (2017).

399 21. Majumdar, G. *et al.* Genome-Wide Transposon Mutagenesis in *Mycobacterium tuberculosis* and
400 *Mycobacterium smegmatis*. *Methods Mol. Biol.* **1498**, 321–335 (2017).

401 22. Dubos, R. J. & Davis, B. D. Factors affecting the growth of tubercle bacilli in liquid media. *J. Exp. Med.*
402 **83**, 409–423 (1946).

403 23. Long, J. E. *et al.* Identifying essential genes in *Mycobacterium tuberculosis* by global phenotypic
404 profiling. *Methods Mol. Biol.* **1279**, 79–95 (2015).

405 24. DeJesus, M. A., Ambadipudi, C., Baker, R., Sassetti, C. & Ioerger, T. R. TRANSIT--A Software Tool for
406 *Himar1* TnSeq Analysis. *PLoS Comput. Biol.* **11**, e1004401 (2015).

407 25. DeJesus, M. A. & Ioerger, T. R. A Hidden Markov Model for identifying essential and growth-defect
408 regions in bacterial genomes from transposon insertion sequencing data. *BMC Bioinformatics* **14**,
409 (2013).

410 26. Zaykin, D. V., Zhivotovsky, L. A., Westfall, P. H. & Weir, B. S. Truncated product method for
411 combining P-values. *Genet. Epidemiol.* **22**, 170–185 (2002).

412 27. Matern, W. & Jenquin, R. Github: [joelbader/essential_genes](https://github.com/joelbader/essential_genes) v1.1. (2019).
413 doi:10.5281/zenodo.3337213
414

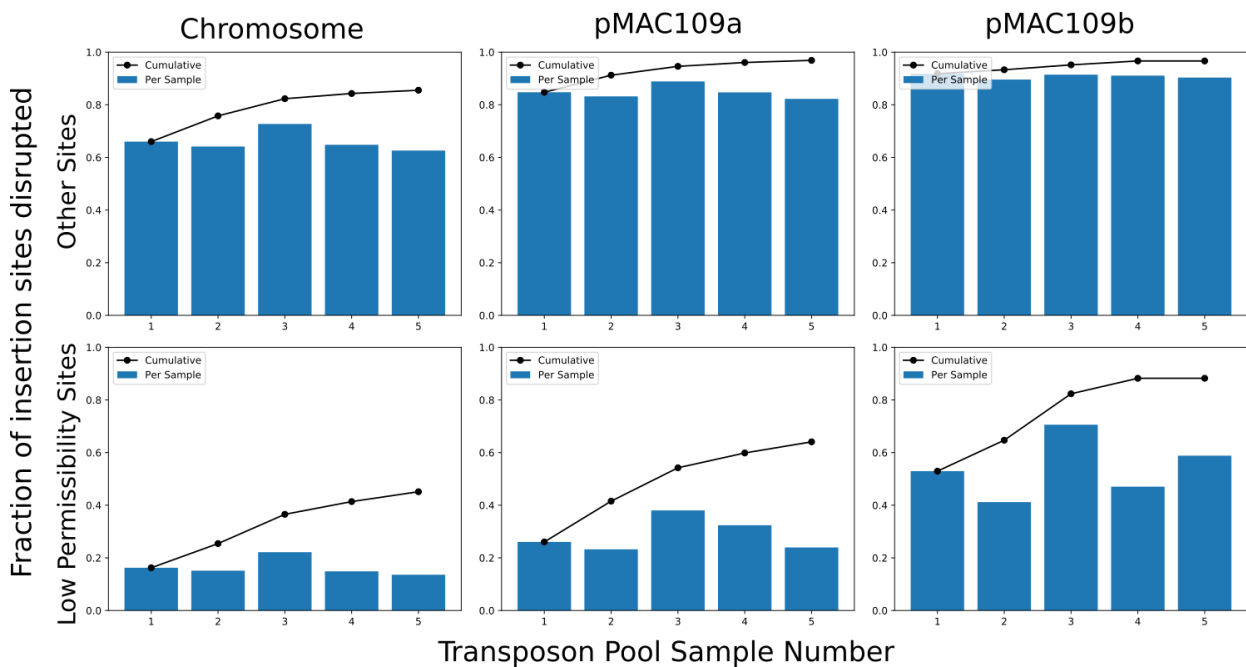
415 **Tables:**

416 **Table 1:** Table of features annotated by our analysis method. NE = No Effect, GD = Growth Defect, ES =
417 Essential, GA = Growth Advantage, N/A = Feature lacks potential insertion sites (TA dinucleotide) for the
418 Himar1 transposon or only contains sites shared with another feature.

	CDS	Pseudogene	tRNA	Riboswitch	rRNA	ncRNA	tmRNA
NE	2850	117	8	5	2	1	0
ES	259	0	8	0	2	0	1
GD	1208	32	26	0	0	1	0
GA	460	29	0	0	0	0	0
N/A	64	13	4	1	0	0	0

419

420 **Figures:**

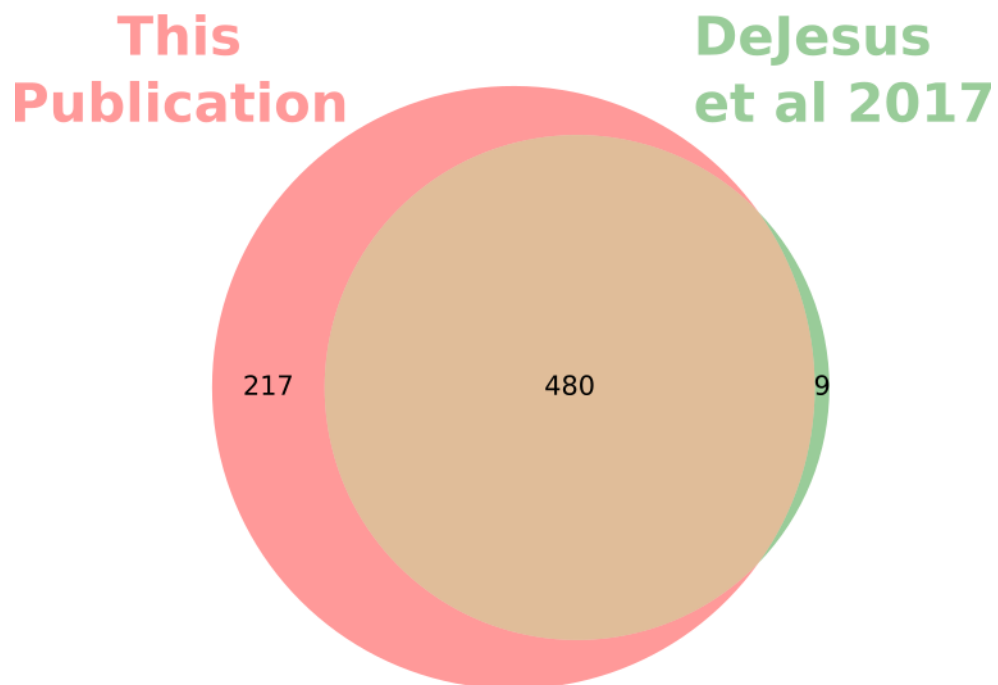


421

422 **Figure 1:** Each barplot shows the fraction of potential Himar1 insertion sites (TA dinucleotide) observed
423 to have sustained at least one insertion in each independent pool of mutants for each replicon of the
424 MAC109 genome. The line plots indicate the cumulative fraction of occupied insertion sites. Notably, the

425 fraction of unique sites occupied saturates for sites not matching the previously defined sequence motif
426 for low permissibility sites ([CG]GNTANC[CG]). However, sites matching this motif can be seen to be
427 near saturation only in the case of the small plasmid (pMAC109b).

428



429

430 **Figure 2:** Venn diagram of essential genes predictions for *Mycobacterium tuberculosis* strain H37Rv from
431 our analysis compared to the previously published essential gene predictions from DeJesus et al ⁷.
432 Notably, the genes labelled essential by the HMM are nearly a subset of the genes labelled as essential
433 by our method. Only protein coding sequences are considered in this diagram.

434

435 **Figure S1:** Simulated data showing correctness of rank-based filter. As described, simulated read counts
436 were generated to test our rank-based filter procedure. A simulation of either 5 sequenced samples ((A)
437 and (B)) or 50 samples ((C) and (D)) was generated. (A) and (C) show histograms of the read counts

438 across all sites before applying the filter procedure in green and the read counts after applying the filter
439 procedure in blue. In red we plot the pmf of our sampling distribution for the null distributed sites.
440 Performance was assessed by q-q plots in (B) and (D). In green are the empirical quantiles before
441 applying the rank-based filter procedure and in blue are the quantiles after filtering. The red line
442 represents perfect theoretical performance.

443 **Descriptions of supplemental files:**

444 • Supplemental Figure S1: Simulated data showing correctness of rank-based filter
445 • Supplemental Text S1: Protocol for preparing sequencing libraries
446 • Supplemental Text S2: Additional details of analysis method
447 • Supplemental Table S1: Transformation efficiency of avium strains.
448 • Supplemental Table S2: Gene prediction in MAC109 (with p-values and LFC)
449 • Supplemental Table S3: Raw data in MAC109 along with gene predictions
450 • Supplemental Table S4: Essential genes in H37Rv based on previous data
451 • Supplemental Table S5: Overlap between MAC109 and Mtb essential genes (both computed
452 with our analysis method)

453